ISSN 1726-5749

SENSORS & TRANSDUCERS

12/11 vol. 13 Special

MEMS & NEMS: Design, Fabrication and Applications

International Frequency Sensor Association Publishing

Sensors & Transducers

Volume 13, Issue 12
December 2011

www.sensorsportal.com

ISSN 1726-5479

Editors-in-Chief: Sergey Y. Yurish, tel.: +34 93 413 7941, e-mail: editor@sensorsportal.com
Guest Editors: Elena Gaura, James Brusey, and Ramona Rednic

Editors for Western Europe
Meijer, Gerard C.M., Delft University of Technology, The Netherlands
Ferrari, Vittorio, Universitá di Brescia, Italy

Editor for Eastern Europe
Sachenko, Anatoly, Ternopil State Economic University, Ukraine

Editors for North America
Datskos, Panos G., Oak Ridge National Laboratory, USA
Fabien, J. Josse, Marquette University, USA
Katz, Evgeny, Clarkson University, USA

Editor South America
Costa-Felix, Rodrigo, Inmetro, Brazil

Editor for Africa
Maki K.Habib, American University in Cairo, Egypt

Editor for Asia
Ohyama, Shinji, Tokyo Institute of Technology, Japan

Editor for Asia-Pacific
Mukhopadhyay, Subhas, Massey University, New Zealand

Editorial Advisory Board

Abdul Rahim, Ruzairi, Universiti Teknologi, Malaysia
Ahmad, Mohd Noor, Nothern University of Engineering, Malaysia
Annamalai, Karthigeyan, National Institute of Advanced Industrial Science and Technology, Japan
Arcega, Francisco, University of Zaragoza, Spain
Arguel, Philippe, CNRS, France
Ahn, Jae-Pyoung, Korea Institute of Science and Technology, Korea
Arndt, Michael, Robert Bosch GmbH, Germany
Ascoli, Giorgio, George Mason University, USA
Atalay, Selcuk, Inonu University, Turkey
Atghiaee, Ahmad, University of Tehran, Iran
Augutis, Vygantas, Kaunas University of Technology, Lithuania
Avachit, Patil Lalchand, North Maharashtra University, India
Ayesh, Aladdin, De Montfort University, UK
Azamimi, Azian binti Abdullah, Universiti Malaysia Perlis, Malaysia
Bahreyni, Behraad, University of Manitoba, Canada
Baliga, Shankar, B., General Monitors Transnational, USA
Baoxian, Ye, Zhengzhou University, China
Barford, Lee, Agilent Laboratories, USA
Barlingay, Ravindra, RF Arrays Systems, India
Basu, Sukumar, Jadavpur University, India
Beck, Stephen, University of Sheffield, UK
Ben Bouzid, Sihem, Institut National de Recherche Scientifique, Tunisia
Benachaiba, Chellali, Universitaire de Bechar, Algeria
Binnie, T. David, Napier University, UK
Bischoff, Gerlinde, Inst. Analytical Chemistry, Germany
Bodas, Dhananjay, IMTEK, Germany
Borges Carval, Nuno, Universidade de Aveiro, Portugal
Bousbia-Salah, Mounir, University of Annaba, Algeria
Bouvet, Marcel, CNRS – UPMC, France
Brudzewski, Kazimierz, Warsaw University of Technology, Poland
Cai, Chenxin, Nanjing Normal University, China
Cai, Qingyun, Hunan University, China
Campanella, Luigi, University La Sapienza, Italy
Carvalho, Vitor, Minho University, Portugal
Cecelja, Franjo, Brunel University, London, UK
Cerda Belmonte, Judith, Imperial College London, UK
Chakrabarty, Chandan Kumar, Universiti Tenaga Nasional, Malaysia
Chakravorty, Dipankar, Association for the Cultivation of Science, India
Changhai, Ru, Harbin Engineering University, China
Chaudhari, Gajanan, Shri Shivaji Science College, India
Chavali, Murthy, N.I. Center for Higher Education, (N.I. University), India
Chen, Jiming, Zhejiang University, China
Chen, Rongshun, National Tsing Hua University, Taiwan
Cheng, Kuo-Sheng, National Cheng Kung University, Taiwan
Chiang, Jeffrey (Cheng-Ta), Industrial Technol. Research Institute, Taiwan
Chiriac, Horia, National Institute of Research and Development, Romania
Chowdhuri, Arijit, University of Delhi, India
Chung, Wen-Yaw, Chung Yuan Christian University, Taiwan
Corres, Jesus, Universidad Publica de Navarra, Spain
Cortes, Camilo A., Universidad Nacional de Colombia, Colombia
Courtois, Christian, Universite de Valenciennes, France
Cusano, Andrea, University of Sannio, Italy
D'Amico, Arnaldo, Università di Tor Vergata, Italy
De Stefano, Luca, Institute for Microelectronics and Microsystem, Italy
Deshmukh, Kiran, Shri Shivaji Mahavidyalaya, Barshi, India
Dickert, Franz L., Vienna University, Austria
Dieguez, Angel, University of Barcelona, Spain
Dighavkar, C. G., M.G. Vidyamandir's L. V.H. College, India
Dimitropoulos, Panos, University of Thessaly, Greece
Ko, Sang Choon, Electronics. and Telecom. Research Inst., Korea South
Ding, Jianning, Jiangsu Polytechnic University, China
Djordjevich, Alexandar, City University of Hong Kong, Hong Kong
Donato, Nicola, University of Messina, Italy
Donato, Patricio, Universidad de Mar del Plata, Argentina
Dong, Feng, Tianjin University, China
Drljaca, Predrag, Instersema Sensoric SA, Switzerland
Dubey, Venketesh, Bournemouth University, UK
Enderle, Stefan, Univ.of Ulm and KTB Mechatronics GmbH, Germany
Erdem, Gursan K. Arzum, Ege University, Turkey
Erkmen, Aydan M., Middle East Technical University, Turkey
Estelle, Patrice, Insa Rennes, France
Estrada, Horacio, University of North Carolina, USA
Faiz, Adil, INSA Lyon, France
Fericean, Sorin, Balluff GmbH, Germany
Fernandes, Joana M., University of Porto, Portugal
Francioso, Luca, CNR-IMM Institute for Microelectronics and Microsystems, Italy
Francis, Laurent, University Catholique de Louvain, Belgium
Fu, Weiling, South-Western Hospital, Chongqing, China
Gaura, Elena, Coventry University, UK
Geng, Yanfeng, China University of Petroleum, China
Gole, James, Georgia Institute of Technology, USA
Gong, Hao, National University of Singapore, Singapore
Gonzalez de la Rosa, Juan Jose, University of Cadiz, Spain
Granel, Annette, Goteborg University, Sweden
Graff, Mason, The University of Texas at Arlington, USA
Guan, Shan, Eastman Kodak, USA
Guillet, Bruno, University of Caen, France
Guo, Zhen, New Jersey Institute of Technology, USA
Gupta, Narendra Kumar, Napier University, UK
Hadjiloucas, Sillas, The University of Reading, UK
Haider, Mohammad R., Sonoma State University, USA
Hashsham, Syed, Michigan State University, USA
Hasni, Abdelhafid, Bechar University, Algeria
Hernandez, Alvaro, University of Alcala, Spain
Hernandez, Wilmar, Universidad Politecnica de Madrid, Spain
Homentcovschi, Dorel, SUNY Binghamton, USA
Horstman, Tom, U.S. Automation Group, LLC, USA
Hsiai, Tzung (John), University of Southern California, USA
Huang, Jeng-Sheng, Chung Yuan Christian University, Taiwan
Huang, Star, National Tsing Hua University, Taiwan
Huang, Wei, PSG Design Center, USA
Hui, David, University of New Orleans, USA
Jaffrezic-Renault, Nicole, Ecole Centrale de Lyon, France
Jaime Calvo-Galleg, Jaime, Universidad de Salamanca, Spain
James, Daniel, Griffith University, Australia
Janting, Jakob, DELTA Danish Electronics, Denmark
Jiang, Liudi, University of Southampton, UK
Jiang, Wei, University of Virginia, USA
Jiao, Zheng, Shanghai University, China
John, Joachim, IMEC, Belgium
Kalach, Andrew, Voronezh Institute of Ministry of Interior, Russia
Kang, Moonho, Sunmoon University, Korea South
Kaniusas, Eugenijus, Vienna University of Technology, Austria
Katake, Anup, Texas A&M University, USA
Kausel, Wilfried, University of Music, Vienna, Austria
Kavasoglu, Nese, Mugla University, Turkey
Ke, Cathy, Tyndall National Institute, Ireland
Khelfaoui, Rachid, Université de Bechar, Algeria
Khan, Asif, Aligarh Muslim University, Aligarh, India
Kim, Min Young, Kyungpook National University, Korea South
Sandacci, Serghei, Sensor Technology Ltd., UK

Kotulska, Malgorzata, Wroclaw University of Technology, Poland
Kockar, Hakan, Balikesir University, Turkey
Kong, Ing, RMIT University, Australia
Kratz, Henrik, Uppsala University, Sweden
Krishnamoorthy, Ganesh, University of Texas at Austin, USA
Kumar, Arun, University of South Florida, USA
Kumar, Subodh, National Physical Laboratory, India
Kung, Chih-Hsien, Chang-Jung Christian University, Taiwan
Lacnjevac, Caslav, University of Belgrade, Serbia
Lay-Ekuakille, Aime, University of Lecce, Italy
Lee, Jang Myung, Pusan National University, Korea South
Lee, Jun Su, Amkor Technology, Inc. South Korea
Lei, Hua, National Starch and Chemical Company, USA
Li, Fengyuan (Thomas), Purdue University, USA
Li, Genxi, Nanjing University, China
Li, Hui, Shanghai Jiaotong University, China
Li, Xian-Fang, Central South University, China
Li, Yuefa, Wayne State University, USA
Liang, Yuanchang, University of Washington, USA
Liawruangrath, Saisunee, Chiang Mai University, Thailand
Liew, Kim Meow, City University of Hong Kong, Hong Kong
Lin, Hermann, National Kaohsiung University, Taiwan
Lin, Paul, Cleveland State University, USA
Linderholm, Pontus, EPFL - Microsystems Laboratory, Switzerland
Liu, Aihua, University of Oklahoma, USA
Liu Changgeng, Louisiana State University, USA
Liu, Cheng-Hsien, National Tsing Hua University, Taiwan
Liu, Songqin, Southeast University, China
Lodeiro, Carlos, University of Vigo, Spain
Lorenzo, Maria Encarnacio, Universidad Autonoma de Madrid, Spain
Lukaszewicz, Jerzy Pawel, Nicholas Copernicus University, Poland
Ma, Zhanfang, Northeast Normal University, China
Majstorovic, Vidosav, University of Belgrade, Serbia
Malyshev, V.V., National Research Centre 'Kurchatov Institute', Russia
Marquez, Alfredo, Centro de Investigacion en Materiales Avanzados, Mexico
Matay, Ladislav, Slovak Academy of Sciences, Slovakia
Mathur, Prafull, National Physical Laboratory, India
Maurya, D.K., Institute of Materials Research and Engineering, Singapore
Mekid, Samir, University of Manchester, UK
Melnyk, Ivan, Photon Control Inc., Canada
Mendes, Paulo, University of Minho, Portugal
Mennell, Julie, Northumbria University, UK
Mi, Bin, Boston Scientific Corporation, USA
Minas, Graca, University of Minho, Portugal
Moghavvemi, Mahmoud, University of Malaya, Malaysia
Mohammadi, Mohammad-Reza, University of Cambridge, UK
Molina Flores, Esteban, Benemérita Universidad Autónoma de Puebla, Mexico
Moradi, Majid, University of Kerman, Iran
Morello, Rosario, University "Mediterranea" of Reggio Calabria, Italy
Mounir, Ben Ali, University of Sousse, Tunisia
Mrad, Nezih, Defence R&D, Canada
Mulla, Imtiaz Sirajuddin, National Chemical Laboratory, Pune, India
Nabok, Aleksey, Sheffield Hallam University, UK
Neelamegam, Periasamy, Sastra Deemed University, India
Neshkova, Milka, Bulgarian Academy of Sciences, Bulgaria
Oberhammer, Joachim, Royal Institute of Technology, Sweden
Ould Lahoucine, Cherif, University of Guelma, Algeria
Pamidighanta, Sayanu, Bharat Electronics Limited (BEL), India
Pan, Jisheng, Institute of Materials Research & Engineering, Singapore
Park, Joon-Shik, Korea Electronics Technology Institute, Korea South
Penza, Michele, ENEA C.R., Italy
Pereira, Jose Miguel, Instituto Politecnico de Setebal, Portugal
Petsev, Dimiter, University of New Mexico, USA
Pogacnik, Lea, University of Ljubljana, Slovenia
Post, Michael, National Research Council, Canada
Prance, Robert, University of Sussex, UK
Prasad, Ambika, Gulbarga University, India
Prateepasen, Asa, Kingmoungut's University of Technology, Thailand
Pullini, Daniele, Centro Ricerche FIAT, Italy
Pumera, Martin, National Institute for Materials Science, Japan
Radhakrishnan, S. National Chemical Laboratory, Pune, India
Rajanna, K., Indian Institute of Science, India
Ramadan, Qasem, Institute of Microelectronics, Singapore
Rao, Basuthkar, Tata Inst. of Fundamental Research, India
Raoof, Kosai, Joseph Fourier University of Grenoble, France
Rastogi Shiva, K. University of Idaho, USA
Reig, Candid, University of Valencia, Spain
Restivo, Maria Teresa, University of Porto, Portugal
Robert, Michel, University Henri Poincare, France
Rezazadeh, Ghader, Urmia University, Iran
Royo, Santiago, Universitat Politecnica de Catalunya, Spain
Rodriguez, Angel, Universidad Politecnica de Cataluna, Spain
Rothberg, Steve, Loughborough University, UK
Sadana, Ajit, University of Mississippi, USA
Sadeghian Marnani, Hamed, TU Delft, The Netherlands
Sapozhnikova, Ksenia, D.I.Mendeleyev Institute for Metrology, Russia
Saxena, Vibha, Bhbha Atomic Research Centre, Mumbai, India
Schneider, John K., Ultra-Scan Corporation, USA
Sengupta, Deepak, Advance Bio-Photonics, India
Seif, Selemani, Alabama A & M University, USA
Seifter, Achim, Los Alamos National Laboratory, USA
Shah, Kriyang, La Trobe University, Australia
Sankarraj, Anand, Detector Electronics Corp., USA
Silva Girao, Pedro, Technical University of Lisbon, Portugal
Singh, V. R., National Physical Laboratory, India
Slomovitz, Daniel, UTE, Uruguay
Smith, Martin, Open University, UK
Soleymanpour, Ahmad, Damghan Basic Science University, Iran
Somani, Prakash R., Centre for Materials for Electronics Technol., India
Srinivas, Talabattula, Indian Institute of Science, Bangalore, India
Srivastava, Arvind K., NanoSonix Inc., USA
Stefan-van Staden, Raluca-Ioana, University of Pretoria, South Africa
Stefanescu, Dan Mihai, Romanian Measurement Society, Romania
Sumriddetchka, Sarun, National Electronics and Computer Technology Center, Thailand
Sun, Chengliang, Polytechnic University, Hong-Kong
Sun, Dongming, Jilin University, China
Sun, Junhua, Beijing University of Aeronautics and Astronautics, China
Sun, Zhiqiang, Central South University, China
Suri, C. Raman, Institute of Microbial Technology, India
Sysoev, Victor, Saratov State Technical University, Russia
Szewczyk, Roman, Industrial Research Inst. for Automation and Measurement, Poland
Tan, Ooi Kiang, Nanyang Technological University, Singapore,
Tang, Dianping, Southwest University, China
Tang, Jaw-Luen, National Chung Cheng University, Taiwan
Teker, Kasif, Frostburg State University, USA
Thirunavukkarasu, I., Manipal University Karnataka, India
Thumbavanam Pad, Kartik, Carnegie Mellon University, USA
Tian, Gui Yun, University of Newcastle, UK
Tsiantos, Vassilios, Technological Educational Institute of Kaval, Greece
Tsigara, Anna, National Hellenic Research Foundation, Greece
Twomey, Karen, University College Cork, Ireland
Valente, Antonio, University, Vila Real, - U.T.A.D., Portugal
Vanga, Raghav Rao, Summit Technology Services, Inc., USA
Vaseashta, Ashok, Marshall University, USA
Vazquez, Carmen, Carlos III University in Madrid, Spain
Vieira, Manuela, Instituto Superior de Engenharia de Lisboa, Portugal
Vigna, Benedetto, STMicroelectronics, Italy
Vrba, Radimir, Brno University of Technology, Czech Republic
Wandelt, Barbara, Technical University of Lodz, Poland
Wang, Jiangping, Xi'an Shiyou University, China
Wang, Kedong, Beihang University, China
Wang, Liang, Pacific Northwest National Laboratory, USA
Wang, Mi, University of Leeds, UK
Wang, Shinn-Fwu, Ching Yun University, Taiwan
Wang, Wei-Chih, University of Washington, USA
Wang, Wensheng, University of Pennsylvania, USA
Watson, Steven, Center for NanoSpace Technologies Inc., USA
Weiping, Yan, Dalian University of Technology, China
Wells, Stephen, Southern Company Services, USA
Wolkenberg, Andrzej, Institute of Electron Technology, Poland
Woods, R. Clive, Louisiana State University, USA
Wu, DerHo, National Pingtung Univ. of Science and Technology, Taiwan
Wu, Zhaoyang, Hunan University, China
Xiu Tao, Ge, Chuzhou University, China
Xu, Lisheng, The Chinese University of Hong Kong, Hong Kong
Xu, Sen, Drexel University, USA
Xu, Tao, University of California, Irvine, USA
Yang, Dongfang, National Research Council, Canada
Yang, Shuang-Hua, Loughborough University, UK
Yang, Wuqiang, The University of Manchester, UK
Yang, Xiaoling, University of Georgia, Athens, GA, USA
Yaping Dan, Harvard University, USA
Ymeti, Aurel, University of Twente, Netherland
Yong Zhao, Northeastern University, China
Yu, Haihu, Wuhan University of Technology, China
Yuan, Yong, Massey University, New Zealand
Yufera Garcia, Alberto, Seville University, Spain
Zakaria, Zulkarnay, University Malaysia Perlis, Malaysia
Zagnoni, Michele, University of Southampton, UK
Zamani, Cyrus, Universitat de Barcelona, Spain
Zeni, Luigi, Second University of Naples, Italy
Zhang, Minglong, Shanghai University, China
Zhang, Qintao, University of California at Berkeley, USA
Zhang, Weiping, Shanghai Jiao Tong University, China
Zhang, Wenming, Shanghai Jiao Tong University, China
Zhang, Xueji, World Precision Instruments, Inc., USA
Zhong, Haoxiang, Henan Normal University, China
Zhu, Qing, Fujifilm Dimatix, Inc., USA
Zorzano, Luis, Universidad de La Rioja, Spain
Zourob, Mohammed, University of Cambridge, UK

Sensors & Transducers Journal (ISSN 1726-5479) is a peer review international journal published monthly online by International Frequency Sensor Association (IFSA).
Available in electronic and on CD. Copyright © 2011 by International Frequency Sensor Association. All rights reserved.

Sensors & Transducers Journal

Contents

Volume 13
Special Issue
December 2011

www.sensorsportal.com

ISSN 1726-5479

Research Articles

Foreword
Elena Gaura, James P. Brusey, Ramona Rednic I

Wireless Sensors for Space Applications
William Wilson, Gary Atkinson........ 1

Applications of a Navigation Instrument Based on a Micro-Motor Driven by Photons
Jorge Valenzuela and Samson Mil'shtein 11

Fabrication and Analysis of MEMS Test Structures for Residual Stress Measurement
Akshdeep Sharma, Deepak Bansal, Maninder Kaur, Prem Kumar, Dinesh Kumar, Rina Sharma and K. J. Rangra........ 21

An electro-thermal MEMS Gripper with Large Tip Opening and Holding Force: Design and Characterization
Jay J. Khazaai, H. Qu, M. Shillor and L. Smith 31

Self-alignment of Silicon Chips on Wafers: a Numerical Investigation of the Effect of Spreading and Wetting
Jean Berthier, Kenneth Brakke, Sébastien Mermoz, Loïc Sanchez, Christian Fretigny, Léa Di Cioccio 44

Use of Small-Scale Wind Energy to Power Cellular Communication Equipment
B. Plourde, J. Abraham, G. Mowry, W. Minkowycz........ 53

Superhydrophobic Porous Silicon Surfaces
Paolo Nenzi, Alberto Giacomello, Guido Bolognesi, Mauro Chinappi, Marco Balucani, and Carlo Massimo Casciola........ 62

Increased Bandwidth of Mechanical Energy Harvester
B. Ahmed Seddik, G. Despessse, S. Boisseau, E. Defay........ 73

Simplifying the Design,Analysis, and Layout of a N/MEMS Nanoscale Material Testing Device
Richa Bansal, Jason V. Clark........ 87

A Novel Silicon-based Wideband RF Nano Switch Matrix Cell and the Fabrication of RF Nano Switch Structures
Yi Xiu Yang, Hamood Ur Rahman and Rodica Ramer 98

Carbon Nanomaterials for Optical Absorber Applications
Anupama Kaul, James Coles, Krikor Megerian, Michael Eastwood, Robert Green, Thomas Pagano, Prabhakar Bandaru and Mehmet Dokmeci........ 109

Improved Nanoreinforced Composite Material Bonds with Potential Sensing Capabilities
David Starikov, Clyde A. Price, Michael S. Fischer, Abdelhak Bensaoula, Farouk Attia, Thomas A. Glenn, Mounir Boukadoum 117

Upconverting Phosphor Thermometry for High Temperature Sensing Applications
Xiaomei Guo, Hongzhi Zhao, Huihong Song, Elizabeth Zhang, Christopher Combs, Noel Clemens, Xuesheng Chen, Kewen K. Li, Yingyin K. Zou and Hua Jiang.. 124

A Model for Enhanced Chemiluminescence Reactions in Microchambers Combined to an Active Pixel Sensor
Jean Berthier, Pierre L. Joly, Florence Rivera, Patrice Caillat 131

Antibody Immobilization on Conductive Polymer Coated Nonwoven Fibers for Biosensors
Shannon K. Mcgraw, Michael J. Anderson, Evangelyn C. Alocilja, Patrick J. Marek, Kris J. Senecal, Andre G. Senecal 142

Development of a Capillary-driven, Microfluidic, Nucleic Acid Biosensor
Fei He, Yuhong Wang, Shenquan Jin and Sam R. Nugen 150

Authors are encouraged to submit article in MS Word (doc) and Acrobat (pdf) formats by e-mail: editor@sensorsportal.com
Please visit journal's webpage with preparation instructions: http://www.sensorsportal.com/HTML/DIGEST/Submition.htm

International Frequency Sensor Association (IFSA).

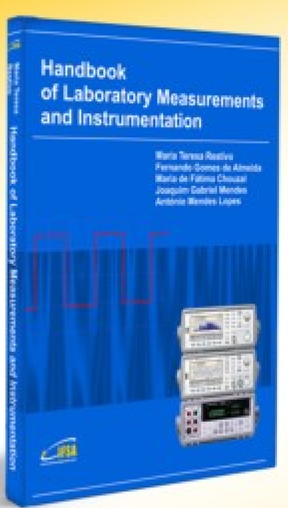

Handbook of Laboratory Measurements and Instrumentation

Maria Teresa Restivo
Fernando Gomes de Almeida
Maria de Fátima Chouzal
Joaquim Gabriel Mendes
António Mendes Lopes

The Handbook of Laboratory Measurements and Instrumentation presents experimental and laboratory activities with an approach as close as possible to reality, even offering remote access to experiments, providing to the reader an excellent tool for learning laboratory techniques and methodologies. Book includes dozens videos, animations and simulations following each of chapters. It makes the title very valued and different from existing books on measurements and instrumentation.

International Frequency Sensor Association Publishing

Order online:
http://www.sensorsportal.com/HTML/BOOKSTORE/Handbook_of_Measurements.htm

The 6th International Conference on Sensor Technologies and Applications

SENSORCOMM 2012

19 - 24 August 2012 - Rome, Italy

Deadline for papers: 5 April 2012

Tracks: Architectures, protocols and algorithms of sensor networks - Energy, management and control of sensor networks - Resource allocation, services, QoS and fault tolerance in sensor networks - Performance, simulation and modelling of sensor networks - Security and monitoring of sensor networks - Sensor circuits and sensor devices - Radio issues in wireless sensor networks - Software, applications and programming of sensor networks - Data allocation and information in sensor networks - Deployments and implementations of sensor networks - Under water sensors and systems - Energy optimization in wireless sensor networks

http://www.iaria.org/conferences2012/SENSORCOMM12.html

The 3rd International Conference on Sensor Device Technologies and Applications

SENSORDEVICES 2012

19 - 24 August 2012 - Rome, Italy

Deadline for papers: 5 April 2012

Tracks: Sensor devices - Ultrasonic and Piezosensors - Photonics - Infrared - Geosensors - Sensor device technologies - Sensors signal conditioning and interfacing circuits - Medical devices and sensors applications - Sensors domain-oriented devices, technologies, and applications - Sensor-based localization and tracking technologies

http://www.iaria.org/conferences2012/SENSORDEVICES12.html

The 5th International Conference on Advances in Circuits, Electronics and Micro-electronics

CENICS 2012

19 - 24 August 2012 - Rome, Italy

Deadline for papers: 5 April 2012

Tracks: Semiconductors and applications - Design, models and languages - Signal processing circuits - Arithmetic computational circuits - Microelectronics - Electronics technologies - Special circuits - Consumer electronics - Application-oriented electronics

http://www.iaria.org/conferences2012/CENICS12.html

Sensors & Transducers Journal, Vol. 13, Special Issue, December 2011, pp. 62-72

Sensors & Transducers

ISSN 1726-5479
© 2011 by IFSA
http://www.sensorsportal.com

Superhydrophobic Porous Silicon Surfaces

[1] Paolo NENZI, [2] Alberto GIACOMELLO, [2] Guido BOLOGNESI,
[3] Mauro CHINAPPI, [1] Marco BALUCANI, and [2] Carlo Massimo CASCIOLA
[1] Dipartimento di Ingegneria dell'Informazione, Elettronica e delle Telecomunicazioni,
[2] Dipartimento di Ingegneria Meccanica e Aerospaziale,
[3] Dipartimento di Fisica, Sapienza Università di Roma, via Eudossiana 18, 00184, Italy
Tel: [1]+39-0644585846, [2]+39-06-44585201
E-mail: [1] balucani@die.uniroma1.it, [2] carlomassimo.casciola@uniroma1.it

Received: 29 June 2011 /Accepted: 16 November 2011 /Published: 28 December 2011

Abstract: In this paper, we present an inexpensive technique to produce superhydrophobic surfaces from porous silicon. Superhydrophobic surfaces are a key technology for their ability to reduce friction losses in microchannels and their self cleaning properties. The morphology of a p-type silicon wafer is modified by an electrochemical wet etch to produce pores with controlled size and distribution and coated with a silane hydrophobic layer. Surface morphology is characterized by means of scanning electron microscope images. Large contact angles are observed on such surfaces and the results are compared with classical wetting models (Cassie and Wenzel) suggesting a mixed Wenzel-Cassie behavior. The presented technique represents a cost-effective means for friction reduction in microfluidic applications, such as lab-on-a-chip. *Copyright © 2011 IFSA.*

Keywords: Macroporous silicon, Hydrophobic coatings, Superhydrophobic surfaces.

1. Introduction

In recent years superhydrophobic surfaces (SHS) [1] have increasingly attracted the interest of the scientific and technological community thanks to their self-cleaning properties and to the large wall-slippage they present for liquid water [2]. Natural SHSs have been observed in plant leaves (Lotus) and insect wings and are characterized by large contact angles, low contact angle hysteresis and large slippage. The typical feature of natural SHSs is their micro/nano scale roughness where air bubbles can get trapped. The presence of the air-water interface is the cause of the surface's low contact angle hysteresis, and slippage. Several research groups have been working towards the development of

synthetic SHSs capable of mimicking the roughness hierarchy of natural SHSs. The air-trapping capability of a surface alone is not enough for SHS application to microfluidics. A crucial issue, indeed, is the stability of the Cassie state [3], since trapped bubbles, under environmental fluctuations, could lead to the transition to the Wenzel state, with water filling completely the roughness elements. A strategy to fulfill this requirement is combining surface morphology modification and hydrophobic coating. The Cassie-Wenzel transition threshold is actually affected by the liquid-solid interface energy which can be significantly reduced by appropriate surface coating, e.g. silane layer deposition. A promising approach to produce robust and economical silicon SHSs is the use of porous silicon [4]. Porous silicon (pSi) is made by crystalline silicon (cSi) anodization in electrolytes (aqueous or organic) containing Hydrofluoric acid (HF). The typical experimental setup is shown in Fig. 1. The morphology of pSi depends from process parameters (mainly the anodization current density and HF concentration in the electrolyte) and spans from 2 nm (nanoporous silicon) up to hundreds of nm (macroporous silicon). The wetting properties of porous silicon strictly depend on the surface morphology, in particular on the pore diameter and porosity. Nanoporous silicon is reportedly highly hydrophilic [5], while macroporous silicon, without surface coatings, can be either highly hydrophobic [5], or hydrophilic, as in this work, depending on the electrolyte and silicon doping type and level. SHSs characterized by contact angles in excess of 150° have been recently obtained from pSi surfaces by morphology modification and/or coating of the surface with a low surface energy layer [5], [6].

In this paper we present an easy-to-implement and economical procedure to realize and characterize macroporous silicon SHSs.

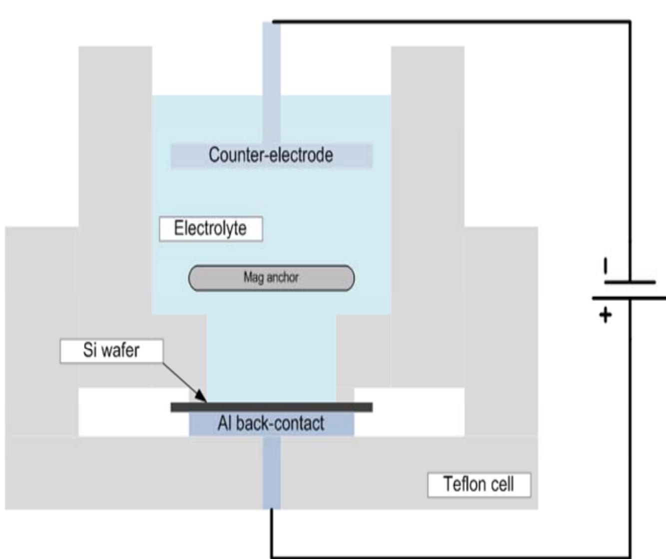

Fig. 1. Electrochemical cell for porous silicon formation.

2. Experimental Section

2.1. Surface Preparation

The sample SHSs are realized, in this work, from 10-20 Ωcm resistivity, boron doped, p-type silicon wafers with {100} orientation. An organic electrolyte, made by mixing HF 48 wt% and Dimethyl sulfoxide (DMSO) with 10:46 ratio has been used to obtain macropores.

Silicon wafers have been cleaned in piranha solution (H_2O_2 (30 %):H_2SO_4 (98 %) 1:3) for 10 minutes, rinsed in deionized water (DI) for 5 minutes and dried with nitrogen. Each wafer has been cut in

square chips of approximately 2.5 cm edge. Silicon chips have been dipped in buffered oxide etch (BOE) solution and rinsed for 5 minutes in DI and dried in nitrogen before being processed.

Each chip is placed in our custom made cell, sketched in Fig. 1. The cell consists of two machined PTFE cylinders that seal the silicon chip, leaving a 1 cm^2 circular surface exposed to the electrolyte. The back of the chip is pressed, by the sealing system, to an aluminum disc that connects it to the external electrical circuit. The circuit is closed via a counter electrode (consisting of a platinum grid) immersed in the electrolyte. A magnetic anchor is used to stir the solution during the anodization process (the cell assembly is placed onto a magnetic stirrer) to remove gas bubbles from the silicon surface and to homogenize the solution. The anodization process is realized by applying a constant current to the silicon chip (the anode) using an AMEL 2055 potentiostat. Immediately after the anodization process, silicon chips are rinsed in DI water for 5 minutes and dried with N_2. The porous surfaces are then activated in an oxygen plasma (50 sccm O_2 at 200 mTorr for 3 minutes) and coated with perfluorooctyltrichlorosilane via low pressure physical vapor deposition (LP-PVD). In addition, the effect of acetone washing on silanized samples is investigated, by performing a 4 min sonication of part of the samples.

2.2. Porous Silicon Morphology

Porous silicon morphology, in particular at the surface, determines its superhydrophobic behavior. The pore morphology depends in general on wafer type, doping density, crystal orientation, electrolyte type, HF concentration in the electrolyte, anodization current density, illumination intensity and anodization time. An extend survey of such morphologies is beyond the scope of this work and the interested reader may find it in [4]. This work concentrates on the study of porous surfaces obtained in HF:DMSO (volume ratio 10:46) organic electrolyte from low-doped p-type silicon wafers. The electrolyte has been chosen to reduce health risks as DMSO is the least dangerous among the solvents used in organic electrolytes for macropore development, the others being Dimethylformamide (DMF) and Acetonitrile (MeCN). The composition of the electrolyte has been optimized to grow stable (non branching), open (not filled by microporous silicon), vertical pores. All processes have been carried in dark. The silicon wafers used in this work can be employed in CMOS processes. Developing a process on CMOS compatible wafers opens the possibility of integrating microfluidic circuits based on SHSs with standard Integrated Circuit (IC) technology. The advantage of such an approach becomes clear when considering the increasing miniaturization of lab-on-a-chip devices that could benefit from electronic control and actuation of microfluidic circuits.

Considering the aforementioned working conditions, the parameter space is reduced to current density and anodization time. We further require pores to have a depth greater than 10 μm, to disfavor the transition to the Wenzel state, as will become clearer in the next section. The mechanism of macropore development on low-doped silicon wafer has been studied in [7], where a growth model is proposed that well agrees with experiments on a broad range of doping levels. Porous silicon formation requires the presence of holes at the silicon-electrolyte interface, the majority carriers in p-type wafers. According to the model in [7], the silicon-electrolyte interface behaves like a Schottky-diode in forward conditions. On silicon side, a space charge region (SCR) not fully depleted of holes, whose width W depends on the built-in potential V_{bi}, silicon doping density N_A, applied bias V_{appl} and the geometry interface. Equation (1) relative to the ideal planar geometry, expresses the SCR width as function of the aforementioned parameters (ε_S=11.8 is the silicon permittivity, E_G=1.12 V is the silicon gap and n_i is the silicon intrinsic carrier concentration):

$$W=\sqrt{\frac{2\varepsilon_0\varepsilon_s(V_{bi}-V_{appl})}{qN_A}}$$

$$V_{bi}=\frac{E_G}{2q}+\frac{kT}{q}\ln\left(\frac{N_A}{n_i}\right) \tag{1}$$

The width of the SCR is minimal at the pore tip due to the geometrical field enhancement while the Schottky barrier height remains constant thus, the majority of the charge transport happens there. The consequence is that depressions in the silicon surface dissolve faster than flat areas, thus producing pores. The charge transport is mainly due to holes diffusion, caused by the concentration gradient of holes near the electrode surface, and involve the entire pore surface. The consequence is that pore walls tend to dissolve but at a slower rate that pores tips. The wall dissolution process stops when the SCRs of adjacent pores join and deplete the walls of holes, ceasing the diffusion current. Detailed analysis of macropore formation physics is reported in [7] and is beyond the scope of this work but the consequences are important for the hydrophobicity of the resulting porous surfaces, in particular:

- Pore starts from pits in the silicon electrode. It is possible to control pore formation by pre-etching pits in the wafer.
- Pore diameter, for a given doping level, is determined by the pore wall thickness between adjacent pores.

In this work, silicon pre-etching has not been performed, as the intent is to produce low cost SHSs. The obtained SHSs are characterized by the presence of two kinds of pores: fully developed pores that extend into the bulk and shallow inter-pores that grow between the former. Inter-pores are depressions that start in the pore walls and extend in the bulk for a few microns. Their growth is suppressed as soon as the development of adjacent pores depletes the wall of holes, thus passivating it against further dissolution.

The porous surfaces have been prepared using three different processes, named *A*, *B* and *C*, reported in Table 1. The highest current density (J_{ps}) has been chosen to be the half of electropolishing threshold, to obtain uniform, reproducible, porous surfaces. The lowest values have been chosen to grow 10 µm deep pores with a process time of 30 minutes to reduce the effect of wall dissolution.

Table 1. Process parameters for the porous silicon surfaces.

Process	J_{ps} [mA/cm^2]	Time [min]
A	5	30
B	10	30
C	15	15

2.3. Contact Angle Measurements

We adopt the sessile drop method to measure the contact angles (CA) over the porous silicon samples. We use a Nikon D7000 camera, equipped with a Micro-Nikkor 60 mm f 2.8/D objective, to record images of millimeter size sessile DI water drops, at rest over horizontal samples. We use freely available software, Drop-Snake [8], to process images and measure contact angles. In Fig. 2 we show some representative results of image analysis. In particular, panels *(a)*-*(c)* show drops sitting on porous silanized samples obtained, respectively with the processes *A*-*C* explained in Table 1. The *(d)* panel, instead, shows a sessile drop on a smooth silane coated silicon wafer.

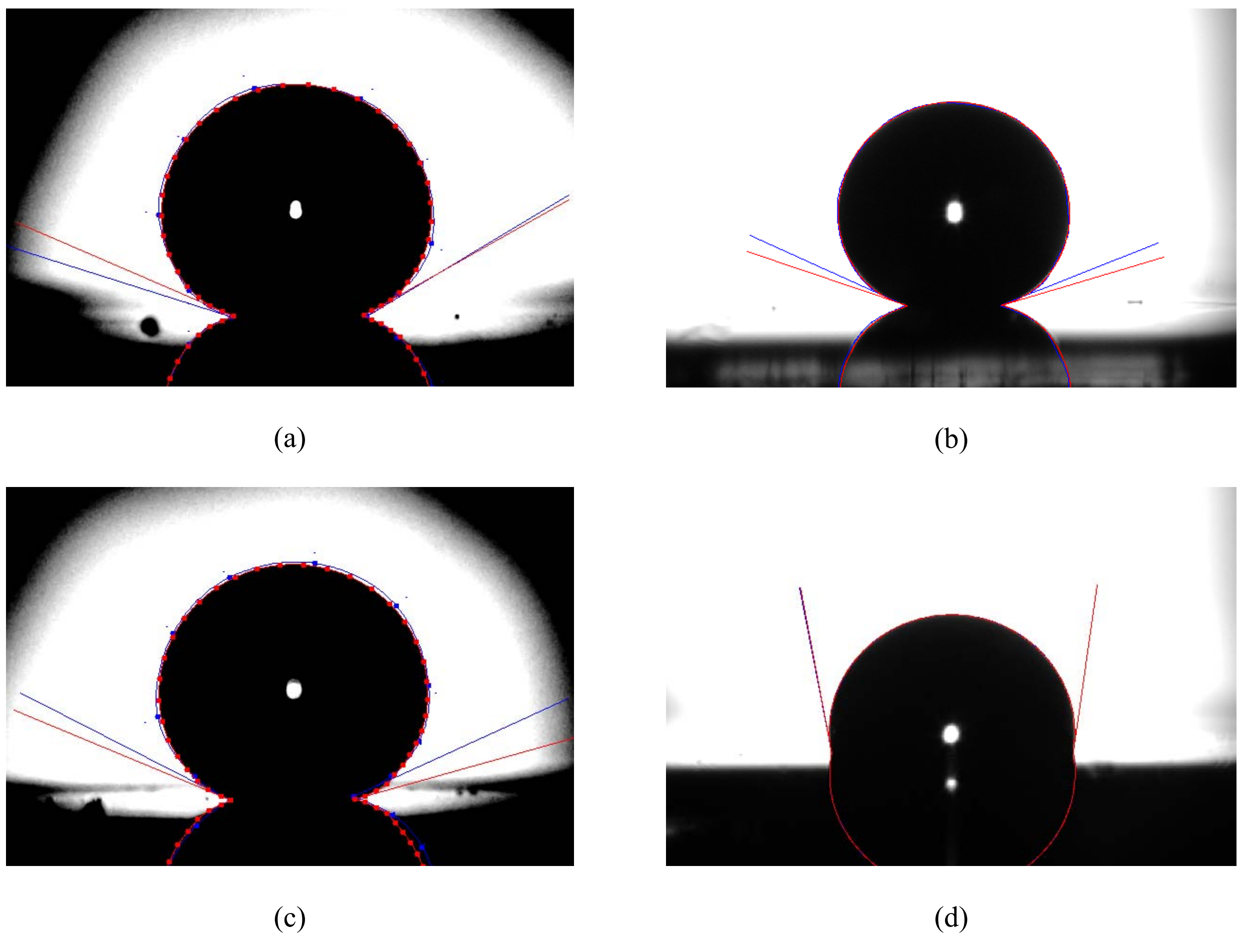

Fig. 2. Contact angles on selected silanized samples: (a) Sample *1*, (b) Sample *2*, (c) Sample *3* as defined in Table 2, corresponding, respectively, to process parameters *A-C* in Table 1; (d) flat silanized wafer.

Table 2. Static contact angles on realized SHSs. The effect of surface morphology (see Table 1 for sample types and Table 3 for pore characteristics) and acetone wash is highlighted.

Sample	Process	Acetone wash	Porous	Contact Angle [°]
1	A	NO	YES	156.0 ± 1.6
2	B	NO	YES	154.5 ± 1.5
3	C	NO	YES	160.8 ± 1.6
4	B	YES	YES	152.8 ± 1.1
5	-	NO	NO	98.5 ± 0.6
6	-	YES	NO	101.8 ± 2.3

The software requires a user-defined detection of the drop boundary (the blue solid line in the figures), which is used as initial guess for the B-spline fitting of the drop boundary. The red solid line is the final computed boundary whence the left and right contact angles are measured. Further details on the software implementation and accuracy may be found in Ref. [8]. The contact angles extracted with Drop-Snake are found to be robust to small changes in the user-defined definition of the drop boundary. The average contact angles are reported in Table 2. We compute the averages by analyzing at least 5 images of a sessile drop on the same sample, recorded after moving the drop on different positions of the observed region. In this way we aim at averaging the effect of local morphology on the contact angle, that is one of the causes of contact angle hysteresis. For the same reason, we average right and left contact angles.

Table 3. Characterization of the surface porosity: Diameter of the pores, area and perimeter as evaluated from top SEM images. Pore depth is evaluated from cross sectional SEM images.

Process	Pore depth [μm]	Pore diameter [μm]	Pore area [μm^2]	Pore Perimeter [μm]	Porosity [%]
A	13.2	1.88 ± 0.53	2.24 ± 0.94	5.77 ± 1.61	55.5 - 61.6
B	14.6	1.84 ± 0.70	1.79 ± 0.89	5.83 ± 2.50	68.8 - 70.6
C	14.3	2.42 ± 0.82	3.28 ± 1.44	7.47 ± 2.69	69.5 - 69.7

2.4. Surface Analysis

Scanning Electron Microscopy (SEM) has been used to characterize the porous surfaces (see Fig. 3).

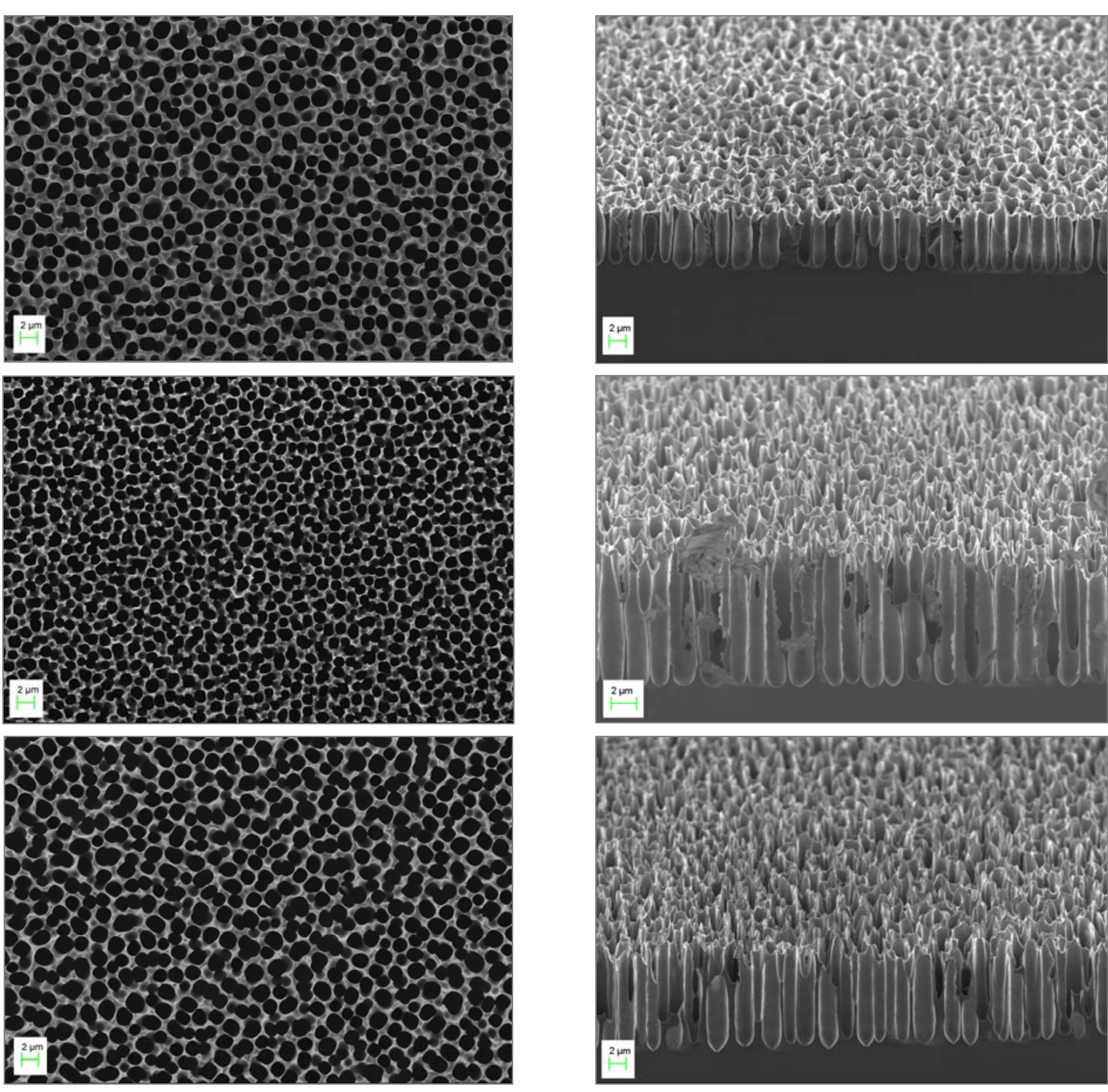

Fig. 3. SEM images of macroporous surfaces (top images on the left column, 63° tilted cross sections on the right) obtained with the processes in Table 1: Images here are ordered from A to C as in the table. The green stroke corresponds to 2 μm.

In particular, all images are obtained from an Auriga FE-SEM produced by Carl Zeiss GmbH. SEM images of macro-porous surfaces have been analyzed using ImageJ [9] software. The porosity value has been computed from the surface topography by counting the percentage of pixels whose intensity is below a set threshold. As can be seen from Fig. 3, fully developed pores appear black with well defined perimeter while shallow pores appear as dark gray areas. The measured porosity is the "surface porosity" of the sample, that is, the area fraction occupied by depressions. This definition differs from the porosity obtained from the gravimetric method [4] that takes into account the bulk porosity, i.e. the mean void fraction of the sample. In this context, mainly concerned with surface interactions, surface porosity is the figure that better describes the interaction with water droplets.

Pore depth has been computed from cross sections of cleaved samples (Fig. 3, right half). All the images were taken at an angle of 63° as this is the maximum angle allowed by the microscope stage.

Some silicon fragments are visible in cross sectional images, due to imperfect cleaving. Sample cross sections clearly show the morphology of pores. Straight, open, pores with uniform depth extend in the silicon bulk.

Cross sections show that, after the porosification process, the silicon fraction far from the surface is still relevant. Furthermore, from top view images, it is evident the continuous structure of the pore walls. Both characteristics contribute to the mechanical stability of the surface. Such an ordered situation does not exist close to the sample surface, as Fig. 4 clearly shows. The presence of inter-pores and the partial dissolution of pore walls confer roughness to the surface, contributing to its hydrophobicity.

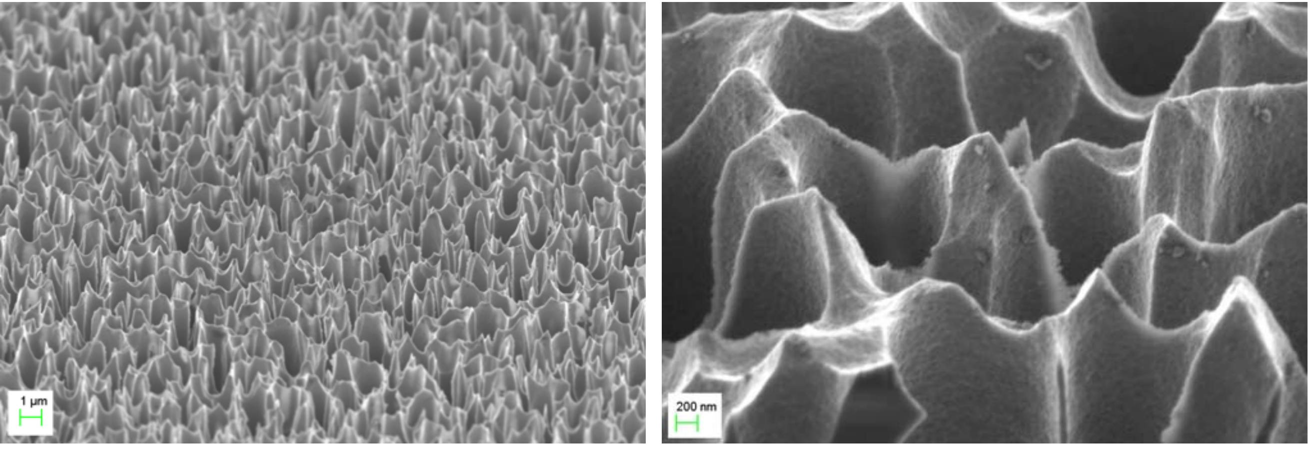

Fig. 4. Surface of the sample obtained with B process (10mA/cm^2, 30 min). Shallow inter-pores are visible as well as the partial dissolution of pore walls.

Three figures have been chosen for surface characterization: pore Feret's diameter, area, and perimeter. The distributions of the parameters have been computed with ImageJ particle analysis tool. We will refer hereafter to diameter with the meaning of maximum Feret's diameter, i.e. the longest dimension of the pore. A summary of surface characteristics, as obtained with the three processes in Table 1, is reported in Table 3. It is noted that the inter-pores dissolution increases with increasing current densities, leading to a spiked surface and pore overlap. As a result the pore perimeter increases and circularity decreases.

3. Results and Discussion

3.1. Surface Characterization

In Table 2 we summarize the contact angle measurements under different experimental conditions, with the aim of investigating the effect of *(i)* surface morphology and *(ii)* low energy coating. We preliminarily note that non-coated samples are hydrophilic, presenting contact angles of 75° on smooth samples and almost total wetting on porous ones. Only contact angles after silanization are reported in Table 2. Cases *1-3* refer to silanized porous surfaces obtained, respectively, with the processes *A-C* of Table 1. For instance, after anodization at 10 mA/cm^2 for 30 minutes (Case *2*) and silanization, the resulting contact angle is 154.5° ± 1.5°. This figure shows that the presented method is successful in providing highly hydrophobic silicon surfaces.

By comparing Cases *1-3*, we note that the sensitivity of contact angles to process parameters -that is, density current and anodization time- is very low. This is due to the fact that, below the electropolishing level, the surface porosity and pore diameter vary only slightly with our free parameters. In view of microfluidic applications, the tolerance on process parameters to obtain SHS with controlled wetting properties is a positive fact.

The evidence that an effective surface energy modification was prompted by the silane PVD is provided by the contact angle of 98.5° ± 0.6° measured over silanized smooth silicon surfaces, corresponding to the static Young angle (Case *5*). This value is in line with the experimental contact angle values reported in [10] for surfaces coated with various silane types. This value is also compatible with that reported in the molecular dynamics simulations of [11] for OTS coated cSi. The influence of surface morphology on the contact angle is reflected in the largely different values reported in for Cases *2* and *5*, and is immediately evident by comparing panels *(b)* and *(d)* in Fig. 2.

The effect of organic solvent washing of the coated samples was tested by performing an acetone sonication of the samples. The cleaning procedure is applied to both porous and smooth silicon surfaces, corresponding to Cases *4* and *6* of Table 2, respectively. Acetone wash may be effective in removing excess silane deposited physically but not grafted on the surface. However, we only detect slight variations in contact angles. A possible explanation of these small variations is the effective cleaning from surface contaminants obtained with the acetone wash.

3.2. Wetting Models

We compare two classical models in order to interpret the reported experimental data in relation to the surface morphology. In particular, the increase of contact angle between porous silicon samples and smooth ones is analyzed in view of Cassie and Wenzel models.

In the Wenzel model, the liquid is assumed to fill in completely the roughness profile. The variation in CA of a rough surface with respect to a perfectly smooth one is ascribed to the larger solid-liquid interface. According to the Wenzel model, the contact angle θ_W is given by

$$\cos\theta_w = r\cos\theta \,, \qquad (2)$$

where r is the ratio of the actually wet area to the projected area of the surface and θ is the Young contact angle on the smooth surface having the same surface composition. In our experiments, the value of θ is computed as an average of Cases *5* and *6* of Table 2.

In the Cassie model, air bubbles are trapped within the pores and the liquid is in contact with the solid only at the peaks of the roughness. The resulting contact angle θ_C is:

$$\cos\theta_c = -1 + \varphi_s (1 + \cos\theta) , \quad (3)$$

where φ_s is the solid fraction of the interface, i.e. the ratio of solid-liquid area to whole droplet base. Though liquid droplets can be observed in both states, the truly superhydrophobic one is the Cassie state which promotes water slippage and low CA hysteresis.

Informed by the analysis of the SEM images in section 2.4, it is possible to provide an estimate r and φ_s. In particular, the φ_s coincides with the complement to unity of the surface porosity χ, that is $\varphi_s = 1 - \chi$. The estimate of r is less straightforward. We consider an ideal surface where each pore is perfectly circular and pores are regularly distributed on a periodic square lattice of size L. In this idealized scheme, we have the following relation between L, φ_s, and R

$$L^2 (1 - \varphi_s) = \pi R^2 , \quad (4)$$

that, after some manipulations, leads to:

$$r = \varphi_s + (1 - \varphi_s)\left(\frac{2h}{R} + 1\right). \quad (5)$$

This expression is still valid if the pores are not on a regular lattice. However, formula (5) is not appropriate in the case that pores overlap. Some overlaps actually happen as apparent in Fig. 2 and the surface morphology is more complicated than the ideal case we are considering, nevertheless Eq. (5) still provides a rough estimation of r.

Using the geometrical characterization of the surfaces in Table 3, along with the average contact angle value measured on smooth silicon surfaces computed from Cases *5* and *6* in Table 2, that is, θ = 100°, we report in Table 4 the predictions for contact angle values corresponding to the models described by Eqs. (2) and (3).

Table 2. Summary of the geometrical features of the surfaces and related classical wetting models predictions for contact angles. The last column reports the wet depth d as obtained from the mixed model in Eq. (6).

Process	r	φ_s	θ_W	θ_C[°]	Penetration [μm]
A	17.44	0.41	non-wetting	131	1.25
B	23.12	0.30	non-wetting	139	0.55
C	17.45	0.30	non-wetting	138	1.01

For all processes, the Wenzel model leads to a left hand side of Eq. (2) smaller than −1. While this value has no direct physical meaning, we can note that the closest physically significant case of $\cos\theta_W = -1$ corresponds to the perfectly hydrophobic state, where the surface is not wet and $\theta_W = 180°$. These considerations suggest that the Wenzel model is not adequate to explain the phenomenology on the considered morphology, and that, reasonably, the roughness profile is not fully wet. This tendency is reasonable in view of the high aspect ratio of the pores that causes the Wenzel state to be extremely energetically unfavorable.
The Cassie equation (3), along with the solid fraction values of Table 4 and the experimental value

θ=100°, yields contact angles in the range θ_C = 130° - 140°, depending on the process details, with the higher values corresponding to the lower solid fractions. However, the experimental contact angles on porous surfaces of Table 2 are larger than the Cassie estimates, while smaller than the perfectly hydrophobic surface towards which the Wenzel model tends. A possible explanation of the discrepancies between the experimental data and the Wenzel and Cassie models may be found in the partial filling of the pores. This phenomenology is intermediate between the limiting cases of the fully wet surface and the "fakir" state, embodied by the Wenzel and Cassie models, respectively.

A simple model for this scenario is now presented. Let us suppose that the pores in regular lattice previously introduced, are filled with water up to a certain depth d. The contact angle is then given by the weighted average of the cosine of contact angles, see [1]:

$$\cos\theta' = \sum \cos\theta_i = \varphi_s \cos\theta + \frac{p \cdot d}{A} \cos\theta - (1 - \varphi_s) . \tag{6}$$

Here p is the total perimeter of the pores and A is the total area of the considered SEM image. Therefore the factor $p \cdot d / A$ corresponds to the ratio between the lateral surface of the pores and the projected area. The first term on the right hand side of Eq. (6) represents the contribution to the average of the liquid-solid interface having contact angle θ. Eventually the third term on the RHS results from the air-liquid interface, as already seen in the Cassie equation. Substituting in Eq. (6) the experimental data θ = *100°* and θ' as in Table 2, we can provide an estimate for the wet depth d. Results for the three process analyzed here are reported in Table 4 and lie around 1 μm. This value appears reasonable in view of the SEM images reported in Fig. 3, but provides only a consistency check on the model.

4. Conclusions

In conclusion, in this paper we presented and characterized an economical microfabrication technique for superhydrophobic surfaces, based on porous silicon. The SHS is realized on a p-type silicon wafer, compatible with CMOS technology, allowing for a potential integration of microfluidics with electronics, in view of the development of lab-on-chip applications. The silane coating proved effective in stabilizing the superhydrophobic Cassie state, allowing for persistent air trapping within the pores. Measured contact angles exceeded 150°. The resistance of the coating to organic solvents was also tested, showing good characteristics. Comparison of contact angle measurements with the available wetting models for heterogeneous surfaces suggested a partial filling of the pores, probably connected to the presence of interpore pitting.

Acknowledgements

We would like to thank Prof. G.P. Romano, Prof. L. Marino, and Mr. P.P. Ciottoli for their help and suggestions with the contact angle measurement setup. SEM scans are performed within the CNIS facilities at the Sapienza University of Rome.

References

[1]. J. Rothstein, Slip on superhydrophobic surfaces, *Annual Review of Fluid Mechanics*, Vol. 42, 2010, pp. 89-109.
[2]. C. Choi, U. Ulmanella, J. Kim, C. Ho, and C. Kim, Effective slip and friction reduction in nanograted superhydrophobic microchannels, *Physics of Fluids*, Vol. 18, 2006, p. 087105.

[3]. A. Cassie and S. Baxter, Wettability of porous surfaces, *Transactions of the Faraday Society*, Vol. 40, 1944, pp. 546-551.
[4]. V. Lehmann, Electrochemistry of silicon, *Wiley Online Library*, 2002.
[5]. A. Ressine, D. Finnskog, G. Marko-Varga, T. Laurell, *NanoBiotechnology*, Vol. 4, 2008, pp. 18-27.
[6]. M. Wang, N. Raghunathan, B. Ziaie, A nonlithographic top-down electrochemical approach for creating hierarchical (micro-nano) superhydrophobic silicon surfaces, *Langmuir*, Vol. 23, 2007, pp. 2300-2303.
[7]. V. Lehmann and S. Rönnenbeck, The Physics of Macropore Formation in Low-Doped p-Type Silicon, *Journal of The Electrochemical Society*, Vol. 146, 1999, pp. 2968-2975.
[8]. A. Stalder, G. Kulik, D. Sage, L. Barbieri, P. Hoffmann, A snake-based approach to accurate determination of both contact points and contact angles, *Colloids and Surfaces A: Physico-chemical and Engineering Aspects*, Vol. 286, 2006, pp. 92-103.
[9]. Rasband, W. S., ImageJ, U. S. National Institutes of Health, Bethesda, Maryland, USA, http://imagej.nih.gov/ij/, 1997-2011
[10]. D. Janssen, R. De Palma, S. Verlaak, P. Heremans, and W. Dehaen, Static solvent contact angle measurements, surface free energy and wettability determination of various self-assembled monolayers on silicon dioxide, *Thin Solid Films*, Vol. 515, 2006, pp. 1433-1438.
[11]. M. Chinappi and C. Casciola, Intrinsic slip on hydrophobic self-assembled monolayer coatings, *Physics of Fluids*, Vol. 22, 2010, p. 042003.

2011 Copyright ©, International Frequency Sensor Association (IFSA). All rights reserved.
(http://www.sensorsportal.com)

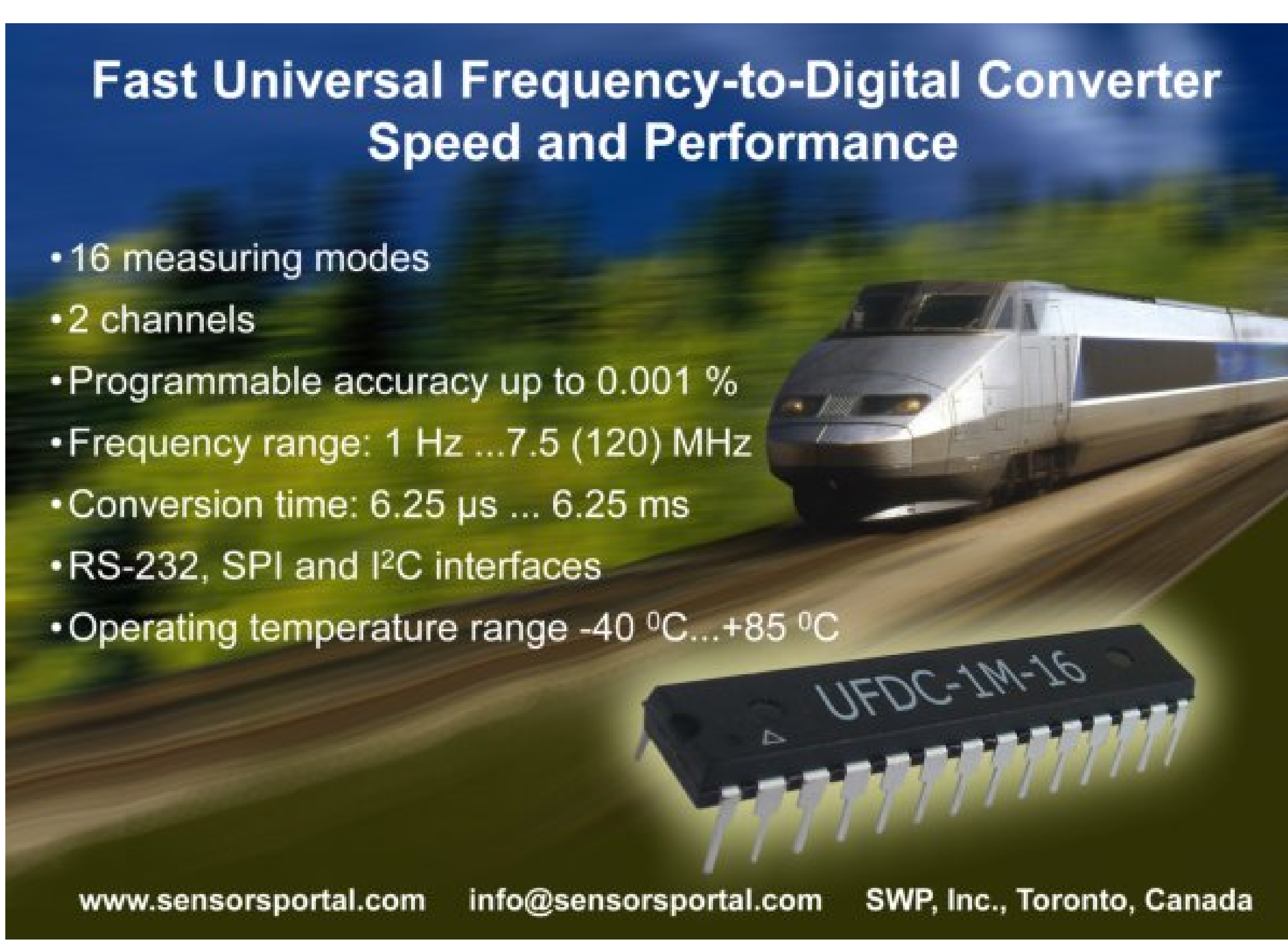

GlobeNet 2012

29 February - 5 March 2012 - Saint Gilles, Reunion Island

IARIA

The Eleventh International Conference on Networks

ICN 2012

Wireless communications:
Satellite, WLL, 4G, Ad Hoc, sensor networks

The Seventh International Conference on Systems

ICONS 2012

System Instrumentation:
Metering embedded sensors; Composing multi-scale measurements; Monitoring instrumentation; Smart sensor-based systems; Calibration and self-calibration systems; Instrumentation for prediction systems

Specialized systems [sensor-based, etc.]:
Sensor-based systems; Biometrics systems; Nano-technology-based systems, etc.

Deadline for papers: 5 October 2011

http://www.iaria.org/conferences2012/GlobeNet12.html

Guide for Contributors

Aims and Scope

Sensors & Transducers Journal (ISSN 1726-5479) provides an advanced forum for the science and technology of physical, chemical sensors and biosensors. It publishes state-of-the-art reviews, regular research and application specific papers, short notes, letters to Editor and sensors related books reviews as well as academic, practical and commercial information of interest to its readership. Because of it is a peer reviewed international journal, papers rapidly published in *Sensors & Transducers Journal* will receive a very high publicity. The journal is published monthly as twelve issues per year by International Frequency Sensor Association (IFSA). In additional, some special sponsored and conference issues published annually. *Sensors & Transducers Journal* is indexed and abstracted very quickly by Chemical Abstracts, IndexCopernicus Journals Master List, Open J-Gate, Google Scholar, etc. Since 2011 the journal is covered and indexed (including a Scopus, Embase, Engineering Village and Reaxys) in Elsevier products.

Topics Covered

Contributions are invited on all aspects of research, development and application of the science and technology of sensors, transducers and sensor instrumentations. Topics include, but are not restricted to:

- Physical, chemical and biosensors;
- Digital, frequency, period, duty-cycle, time interval, PWM, pulse number output sensors and transducers;
- Theory, principles, effects, design, standardization and modeling;
- Smart sensors and systems;
- Sensor instrumentation;
- Virtual instruments;
- Sensors interfaces, buses and networks;
- Signal processing;
- Frequency (period, duty-cycle)-to-digital converters, ADC;
- Technologies and materials;
- Nanosensors;
- Microsystems;
- Applications.

Submission of papers

Articles should be written in English. Authors are invited to submit by e-mail editor@sensorsportal.com 8-14 pages article (including abstract, illustrations (color or grayscale), photos and references) in both: MS Word (doc) and Acrobat (pdf) formats. Detailed preparation instructions, paper example and template of manuscript are available from the journal's webpage: http://www.sensorsportal.com/HTML/DIGEST/Submition.htm Authors must follow the instructions strictly when submitting their manuscripts.

Advertising Information

Advertising orders and enquires may be sent to sales@sensorsportal.com Please download also our media kit: http://www.sensorsportal.com/DOWNLOADS/Media_Kit_2011.pdf

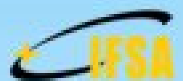

International Frequency Sensor Association Publishing

Digital Sensors and Sensor Systems: Practical Design will greatly benefit undergraduate and at PhD students, engineers, scientists and researchers in both industry and academia. It is especially suited as a reference guide for practicians, working for Original Equipment Manufacturers (OEM) electronics market (electronics/hardware), sensor industry, and using commercial-off-the-shelf components, as well as anyone facing new challenges in technologies, and those involved in the design and creation of new digital sensors and sensor systems, including smart and/or intelligent sensors for physical or chemical, electrical or non-electrical quantities.

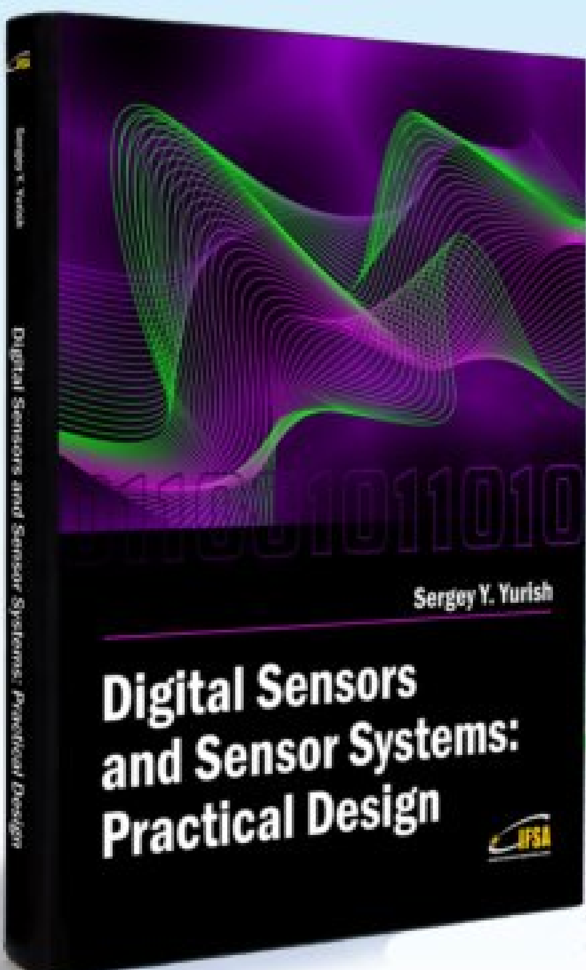

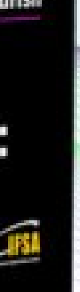

"It is an outstanding and most completed practical guide about how to deal with frequency, period, duty-cycle, time interval, pulse width modulated, phase-shift and pulse number output sensors and transducers and quickly create various low-cost digital sensors and sensor systems …" (from a review)

Order online:
http://www.sensorsportal.com/HTML/BOOKSTORE/Digital_Sensors.htm

www.sensorsportal.com